PRAMANA
— journal of
physics

Vol. 82, No. 5
May 2014
pp. 879–891

Classical simulations of heavy-ion fusion reactions and weakly-bound projectile breakup reactions

S S GODRE
Department of Physics, Veer Narmad South Gujarat University, Surat 395 007, India
E-mail: ssgodre@yahoo.com

DOI: 10.1007/s12043-014-0741-6; ***e*Publication:** 30 April 2014

Abstract. Heavy-ion collision simulations in various classical models are discussed. Heavy-ion reactions with spherical and deformed nuclei are simulated in a classical rigid-body dynamics (CRBD) model which takes into account the reorientation of the deformed projectile. It is found that the barrier parameters depend not only on the initial orientations of the deformed nucleus, but also on the collision energy and the moment of inertia of the deformed nucleus. Maximum reorientation effect occurs at near- and below-barrier energies for light deformed nuclei. Calculated fusion cross-sections for ^{24}Mg + ^{208}Pb reaction are compared with a static-barrier-penetration model (SBPM) calculation to see the effect of reorientation. Heavy-ion reactions are also simulated in a 3-stage classical molecular dynamics (3S-CMD) model in which the rigid-body constraints are relaxed when the two nuclei are close to the barrier thus, taking into account all the rotational and vibrational degrees of freedom in the same calculation. This model is extended to simulate heavy-ion reactions such as ^{6}Li + ^{209}Bi involving the weakly-bound projectile considered as a weakly-bound cluster of deuteron and ^{4}He nuclei, thus, simulating a 3-body system in 3S-CMD model. All the essential features of breakup reactions, such as complete fusion, incomplete fusion, no-capture breakup and scattering are demonstrated.

Keywords. Heavy-ion reactions; classical microscopic approaches; reorientation effect; sub-barrier fusion; breakup reactions.

PACS Nos 25.70.Jj; 24.10.−i; 25.70.De; 25.60.Pj

1. Introduction

Heavy-ion collisions at low energies are dominated by deep-inelastic scattering and fusion which involve large scale transfer of energy from relative motion to internal excitations. It is also well recognized that heavy-ion collisions at energies around the Coulomb barrier are strongly affected by the internal structure of the colliding nuclei [1]. The couplings of the relative motion to the intrinsic degrees of freedom result in a single potential barrier being replaced by a number of distributed barriers. For nuclei with static deformation, the reorientation of the deformed nucleus under the influence of the torque produced by the

long-range Coulomb force may result in modification of the barrier parameters which can be crucial in determining the approach state of the two nuclei for fusion.

In the macroscopic approaches for studying heavy-ion collisions [2–6], one has to choose relevant collective degrees of freedom describing the overall properties of the nuclei and invoke suitable mechanisms for transfer of energy and angular momentum from the collective, to the remaining frozen internal degrees of freedom or by invoking suitable couplings. Quantum mechanical coupled-channel calculations [4–6] have been widely used to study heavy-ion collisions close to the barrier. On the other hand, in a completely microscopic approach, which necessarily involves individual particle degrees of freedom, the energy and angular momentum transfer is in-built through the solution of the time-dependent many-body equations of motion and the relevant collective degrees of freedom are determined by the system itself. Quantum mechanical microscopic approaches such as time-dependent Hartree–Fock (TDHF) [7–12] have been used for studying heavy-ion fusion. However, TDHF calculations are very compute intensive.

Since heavy ions with energies of even a few MeV/nucleon have short de Broglie wavelength compared to the size of the ions, classical approximations are expected to be good for macroscopic features of heavy-ion reactions such as fusion. Therefore, various classical macroscopic and microscopic approaches have also been used for studying heavy-ion reactions [2,3,13–28]. Classical approaches offer clarity of interpretations and computational ease.

Within the classical approximations, it is possible to include all the degrees of freedom in a completely unconstrained microscopic calculation such as classical molecular dynamics model (CMD) [13–22]. However, various levels of approximations are considered to understand the effect of specific degrees of freedom. Models developed with various levels of degrees of freedom are discussed in this paper. The choice of *NN*-potential and construction of the nuclei for collision calculations are discussed in §2. A microscopic static barrier penetration model (SBPM) is discussed in §3. Reorientation effect in heavy-ion collision using the classical rigid-body dynamics model (CRBD) is discussed in detail in §4. Classical molecular dynamics model (CMD) is discussed in §5. A 3-stage CMD model (3S-CMD) which combines CRBD and CMD models is discussed in §6.

While heavy-ion collision in the approach stage is essentially a two-body problem, where each individual nucleus consists of a number of protons and neutrons, in some cases a loosely bound projectile may break up in the vicinity of a heavy target nucleus leading to a heavy-ion collision involving three or more bodies. An extension of the 3S-CMD model to deal with such breakup reactions is discussed in §7. Finally, summary is given in §8.

2. Nuclei in classical approximations

In all the classical calculations, nucleons are assumed to be classical point particles, without spin, interacting with each other via suitable two-body *NN* force. The Coulomb potential between protons has the usual form

$$V^{\mathrm{C}}(r_{ij}) = \frac{1.44}{r_{ij}}(\mathrm{MeV}) \tag{1}$$

and the *NN* potential chosen is a soft-core Gaussian potential of the form [26,29]

$$V^{\mathrm{N}}(r_{ij}) = -V_0\left(1 - \frac{C}{r_{ij}}\right)\exp\left(-\frac{{r_{ij}}^2}{{r_0}^2}\right). \tag{2}$$

The *NN* potential between like particles is taken to be about 20% weaker than that between unlike particles [30].

The distribution of nucleons in each nucleus is first obtained by cyclically minimizing the total potential energy of an initially random distribution of nucleons, with respect to small spatial displacements of individual nucleon coordinates using the code STATIC [26]. The zero-point energy in the ground state is explicitly neglected. However, a purely phenomenological effective *NN* potential is chosen with its parameters adjusted to reproduce binding energy and rms radius for the cluster of particles in the ground state. For the reactions studied in this paper a parameter set called potential P4 of [26] is used ($V_0 = 1155$ MeV, $C = 2.07$ fm, $r_0 = 1.2$ fm).

Final configuration of nucleon positions produces a frozen nucleus. Since for $A \geq 5$ one can have many local minima in the binding energy, a nucleus is chosen which has the maximum binding energy among a large number of such configurations (most-bound nucleus) [31,32] or alternatively a configuration which is close to the experimental ground state properties is chosen [28,33]. Figures 1 and 2 show maximum binding energy and corresponding root-mean-square radius, respectively of many nuclei generated using the STATIC code and potential P4.

3. Static barrier penetration model (SBPM)

The ion–ion potential is obtained as a function of the centre of mass separation (R_{cm}) of the two nuclei in the sudden approximation [27]. The ion–ion potential is the sum of the nuclear and Coulomb potentials between all the nucleons of the two ions. The barrier parameters V_{B} and R_{B} correspond to the outer maximum of the ion–ion potential and ω_{B} corresponds to the second derivative of this peak. This gives barrier parameters of head-on collision for a given orientation of the two nuclei.

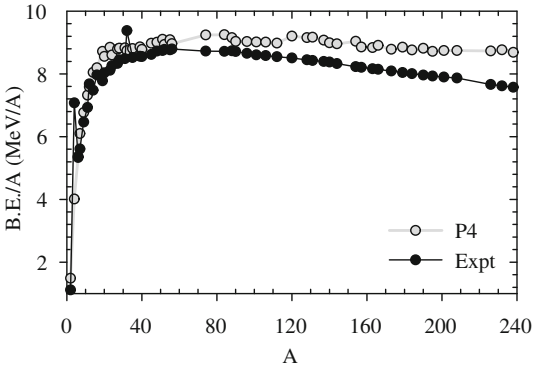

Figure 1. BE/*A* for most-bound nuclei [32].

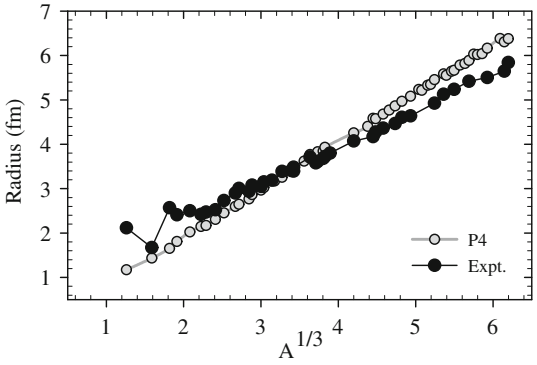

Figure 2. RMS radius for most-bound nuclei [32].

Using barrier parameters corresponding to the given collision energy and considering a large number of randomly chosen initial orientations, orientation-averaged fusion cross-section is calculated using the Wong's formula [34]

$$\sigma(E_{\rm cm}) = \left[\frac{R_{\rm B}^2 \hbar\omega_{\rm B}}{2E_{\rm cm}}\right] \ln\left\{1 + \exp\left(2\pi \frac{E_{\rm cm} - V_{\rm B}}{\hbar\omega_{\rm B}}\right)\right\}. \tag{3}$$

Calculated results show good agreement for fusion cross-sections and barrier distribution for ^{154}Sm + ^{16}O and ^{12}C + ^{232}Th reactions [27]. Although static deformation of nuclei is taken care of, all the degrees of freedom including the rotational degrees of freedom are suppressed and all the dynamical effects are explicitly neglected in this model.

4. Classical molecular dynamics (CMD)

All the degrees of freedom are included in a completely unconstrained microscopic calculation, where trajectories of all the nucleons in both the colliding nuclei are obtained by solving classical coupled equations of motion.

$$m\frac{{\rm d}^2 r_i}{{\rm d}t^2} = \nabla_i \left[\sum_{j\neq i} V_{ij}\right]. \tag{4}$$

This model was earlier used for studying heavy-ion collisions at higher collision energies [13–17] and it was also used to demonstrate its applicability for low-energy heavy-ion collisions in [18,19]. This model has been extensively used to calculate fusion cross-sections at energies above the barrier for ^{16}O+^{16}O and ^{40}Ca+^{40}Ca [26,35]; ^{16}O+^{40}Ca [35]; ^{24}Mg+^{16}O and ^{16}O+^{115}In [36]; ^{27}Al+^{16}O [37] reactions. General features of fusion cross-sections above the barrier energies were reproduced and it was shown that better agreement with cross-sections could be obtained by a suitable choice of parameters of the *NN*-potential [26]. All these calculations took into account the size of the nuclei but did not consider the shape of the constructed nuclei and were initiated at a very small separation of 20 fm.

5. Classical rigid-body dynamics (CRBD) model

This model is developed specifically to study the Coulomb reorientation of deformed nucleus in heavy-ion collision [21,28]. The CRBD model allows rotational and translational degrees of freedom only and all other degrees of freedom are suppressed. This approach is useful in bringing out the importance of reorientation effect which is neglected in SBPM calculation and which would be obscured in CMD calculation because of the presence of other degrees of freedom.

The collision simulation process is initiated by bringing the two nuclei along their Rutherford trajectories with the given collision energy $E_{\rm cm}$ and impact parameter b. The actual model calculation is started at $t = 0$ at a finite but large distance $R_{\rm in}$, where the two nuclei with their ground-state configuration are placed with a given relative orientation between them. $R_{\rm in} = 2500$ fm is chosen to take into account the full effect of the torque produced by the long-range Coulomb force [21]. The nuclei are assumed to be rigid and the orientation of the body-frame axes aligned along the principal axes is determined from the attitude matrix. The origin of the body frame coincides with the centre of mass of each nucleus. At $t = 0$, the two nuclei are assumed to be rotating with zero angular velocity. The motion of the centre of mass and the orientation of the principal axes of the two colliding nuclei are found from the classical equations of motion for rigid bodies [28,38]. The instantaneous orientation of the two nuclei with respect to each other specified by the Euler angles (α, β, γ) defined relative to the reaction plane is as shown in figure 3.

As the two nuclei evolve from $t = 0$, the deformed nucleus (^{24}Mg) experiences torque in the Coulomb field of the heavy (^{208}Pb) nucleus and its orientation changes by a small amount at large separation distances. The overall integrated effect and the large value of the torque at close distances result in appreciable reorientation of the light deformed nucleus. The extent of reorientation can be defined by $\Delta\beta = \beta_f - \beta_0$, where β_f is the angle made by the symmetry axis of ^{24}Mg at $R_{\rm cm}$ close to the barrier top and β_0 is the initial angle at $R_{\rm in} = 2500$ fm. Figure 4a shows the extent of reorientation of ^{24}Mg as a function of β_0 for different collision energies. The extent of reorientation depends not only on the initial orientation but also strongly on the collision energy.

The number of trajectories $N(\beta_f)$ which arrive near the barrier top with an angle β_f are shown in figure 4b. Thus, at energies close to the barrier even though at $t = 0$ the initial distribution of orientations is isotropic; the nuclei evolve to arrive at the barrier top with

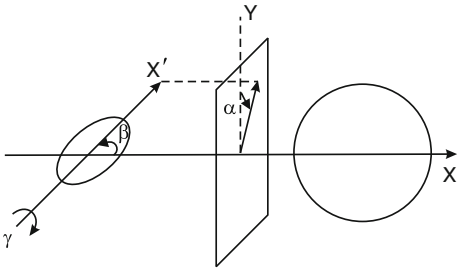

Figure 3. Schematic of the orientation of the body-frame of the deformed nucleus specified by three Euler angles (α, β, γ) relative to the reaction plane [28].

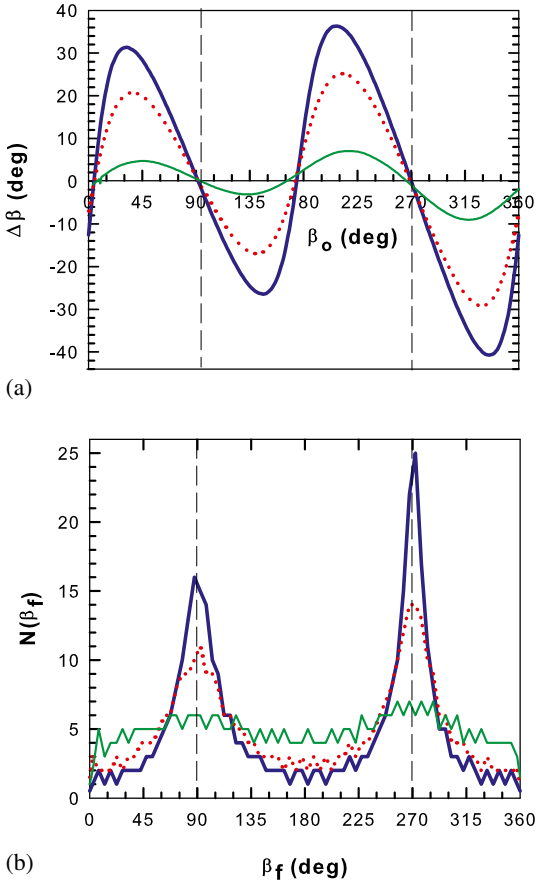

Figure 4. (**a**) Extent of reorientation $\Delta\beta$ for different initial orientation angles β_0. (**b**) The number of trajectories $N(\beta_f)$ with angle β_f for ^{24}Mg + ^{208}Pb collision at $E_{\rm cm} = 115$ MeV (thick solid line), 130 MeV (dotted line) and 250 MeV (thin solid line) [28].

preferred relative orientation, creating an anisotropy in the angular distribution, which is crucial in determining the barrier conditions.

Because of the dynamical effect of reorientation, the barrier parameters are found to depend on the initial orientation and the collision energy. Ion–ion potentials near the barrier top for ^{24}Mg + ^{208}Pb system calculated at different $E_{\rm cm}$, but with the same arbitrary initial orientation, are shown in figure 5. The values of $V_{\rm B}$ and $R_{\rm B}$ depend on the incident energy.

The CRBD calculations of fusion cross-section for ^{24}Mg + ^{208}Pb reaction show suppression of fusion cross-sections at sub-barrier energies as compared to the SBPM calculation [28]. Therefore, it will be of interest to determine the fusion cross-sections for this reaction experimentally at near and below barrier energies.

Figure 6 shows the extent of reorientation $\Delta\beta$ as a function of the initial orientation angle β_0 for ^{154}Sm + ^{16}O and ^{238}U+^{16}O reactions. This figure demonstrates that the

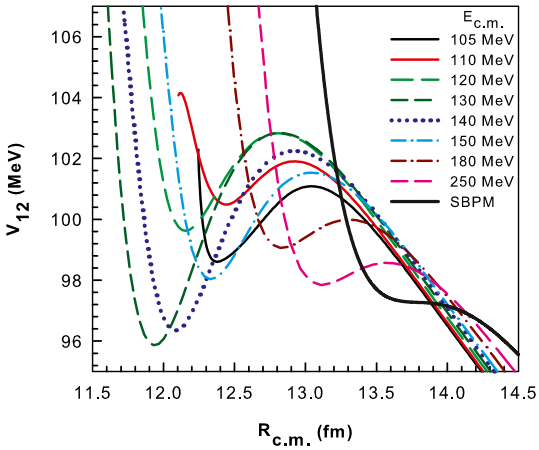

Figure 5. Ion–ion potential for the ^{24}Mg + ^{208}Pb reaction for different collision energies $E_{\rm cm}$ but with the same arbitrary initial orientation in CRBD calculation. Ion–ion potential for this orientation in SBPM calculation is shown by the thick solid line [28].

extent of reorientation also depends on the moment of inertia of the heavy deformed collision partner at energies close to the barrier.

The CRBD calculations show the importance of correctly incorporating the long-range Coulomb torque on the deformed collision partner in collisions at near-barrier energies. The calculations explicitly show that the barrier parameters are not independent of the collision energy, as assumed in some TDHF [7–9] calculations and thus, emphasize the importance of obtaining barrier parameters at every value of $E_{\rm cm}$ for which cross-sections are calculated.

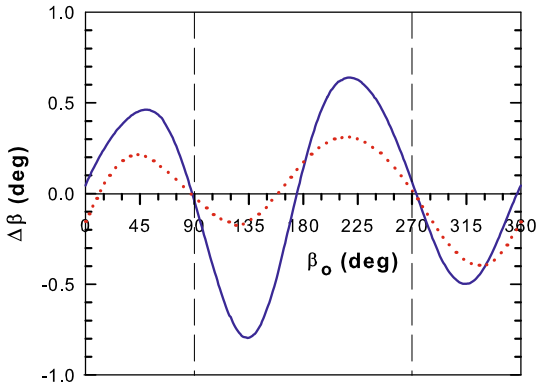

Figure 6. Extent of reorientation $\Delta\beta$ as a function of initial orientation angle β_0 for ^{154}Sm + ^{16}O (solid line) and ^{238}U + ^{16}O (dotted line) reactions with collision energies $E_{\rm cm}$=70 MeV and 90 MeV, respectively [28].

6. 3-stage classical molecular dynamics (3S-CMD) model

In CRBD model calculations, due to the rigid-body constraint, the two nuclei cannot overlap and the energy transfer from relative motion to internal excitation is neglected after crossing the barrier. No bound state is formed between the two nuclei. Passing over the generated fusion barrier is assumed to be resulting in fusion. However, it is desirable to take into account the subsequent capture of the two nuclei behind the fusion barrier. This in effect can modify ω_B, even if V_B and R_B may not get modified substantially, but this in turn can modify the calculated fusion cross-sections.

The above-mentioned problem, in principle, can be overcome by the CMD calculations in which all the degrees of freedom are included and the energy transfer between relative and intrinsic motion is in-built. Dissipation of energy can lead to trapping behind the barrier and result in bound system of the two nuclei. However, the long-range reorientation effect requires initiation of the CMD at large distances (R_{cm} = 2500 fm) like in CRBD calculation. This results in large computational time for each trajectory and accumulation of numerical errors over a very large number of time steps.

To overcome the above-mentioned difficulties and at the same time to take advantage of the CRBD and the CMD model calculations, a 3-stage classical molecular dynamics (3S-CMD) model is recently used for heavy-ion collision simulation which combines both the CRBD and CMD in a common simulation code consecutively [39]. This model explicitly takes into account the long-range reorientation effect as well.

The 3S-CMD model calculation proceeds in the following three stages:

(1) *Rutherford trajectory calculation*: The two nuclei, assumed to be charged point particles, are brought along their Rutherford trajectories with given collision energy and impact parameter up to $R_{cm} = 2500$ fm.
(2) *CRBD model calculation*: The two nuclei (now assumed to be rigid bodies with their ground-state configuration of nucleon positions) are then allowed to evolve further using the CRBD model calculation which is continued up to a relatively small separation of $R_{cm} = 50$ fm.
(3) *CMD calculation*: The rigid-body constraints are relaxed at about $R_{cm} = 50$ fm and trajectories of all the participating nucleons are computed using the coupled Newton's equations of motion for all the particles in a CMD approach.

A simulation of $^{24}Mg + {}^{208}Pb$ collision is carried out in CRBD and 3S-CMD calculations for $E_{cm} = 120$ MeV and $b = 0$. Figure 7 shows calculated T_{cm}, T_{vib} and T_{rot}. Total rotational energy (T_{rot}) in CRBD and 3S-CMD matches well with each other upto distances close to the barrier top; similarly, for total energy of the centre of masses (T_{cm}), thus justifying the use of CRBD model as 2nd stage in the 3S-CMD model. Total internal vibration excitation energy (T_{vib}) rapidly increases, after crossing the barrier top, draining the energy from T_{cm} and resulting in a bound system. Figure 8 shows the ion–ion potential calculated in CRBD and 3S-CMD models. Inside of the barrier is significantly modified by the CMD stage of 3S-CMD. Usual CMD calculation alone, which is initiated only at $R_{cm} = 50$ fm, does not match well (figure 8) with either CRBD or 3S-CMD calculations.

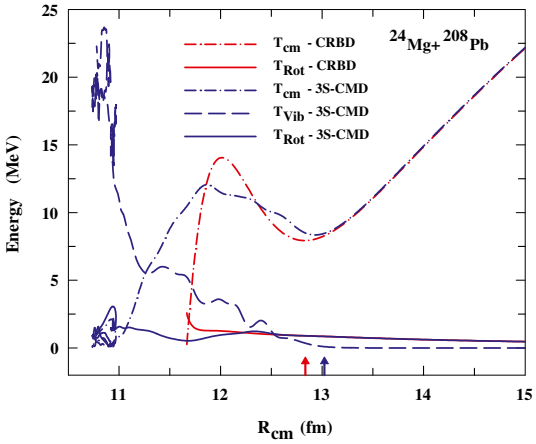

Figure 7. $T_{\rm cm}$, $T_{\rm vib}$ and $T_{\rm rot}$ of ^{24}Mg + ^{208}Pb for CRBD and 3S-CMD [39].

Fusion cross-sections for ^{24}Mg + ^{208}Pb reaction using SBPM, CRBD and 3S-CMD models are shown in figure 9. It can be seen that cross-sections calculated in 3S-CMD are enhanced at lower energies as compared to that corresponding in CRBD calculation.

The 3S-CMD model combines CRBD and CMD seamlessly in a single calculation. It is better than using the CRBD or CMD approach alone. It combines the benefits of both the approaches as 3S-CMD takes both into account; the rotational excitation (reorientation effect) which is a long-range effect and the vibrational excitations which occur close to the barrier or inside of it.

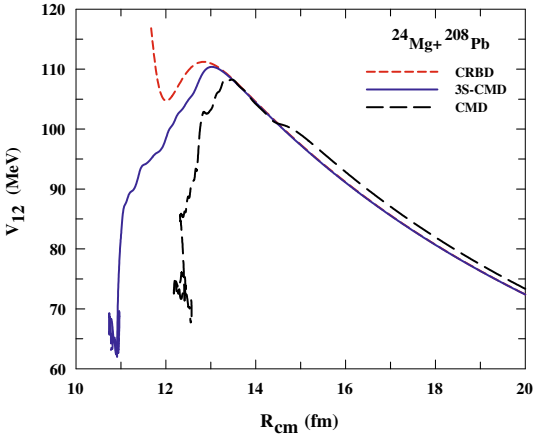

Figure 8. Ion–ion potential of ^{24}Mg + ^{208}Pb for CRBD, 3S-CMD and CMD calculations [39].

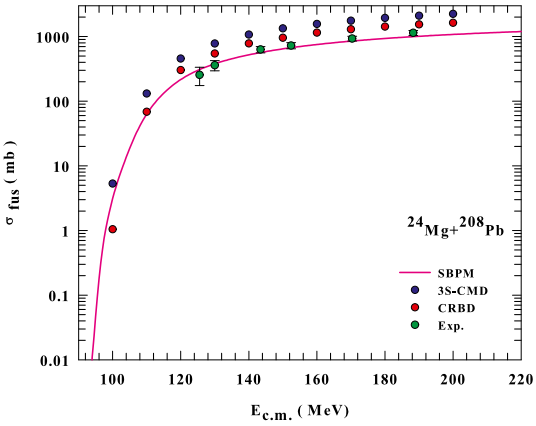

Figure 9. Fusion cross-section for ^{24}Mg + ^{208}Pb system.

7. Weakly-bound projectile breakup reactions (3-body 3S-CMD model)

Heavy-ion fusion reactions above and near the fusion barrier mainly involved tightly bound projectile/target nuclei. But with projectiles such as ^{6,7}Li which are weakly bound, fusion can be affected by their low binding energy, which can cause break up before reaching the fusion barrier. If all the breakup fragments are captured, then it is termed as a complete fusion (CF) and if only some of the fragments are captured, then it is an incomplete fusion (ICF). ICF can change the reaction products, fusion probabilities and distribution of barriers. It is important to understand the effects of breakup of weakly-bound nuclei on the fusion process.

Breakup reactions are studied using continuum discretized couple-channel (CDCC) [40], semiclassical couple channel approximation [24] and classical trajectory model [25].

In the classical trajectory model, the projectile is treated as a two-body system interacting with each other by an assumed weak potential and the breakup is initiated by a breakup probability function. Thus, it is a 3-body classical point–particle system evolving under a given set of interaction potentials between each pair. Deformation and consequent reorientation of the entire projectile system is neglected in this model. The interaction potentials are not obtained self-consistently. The fusion probabilities are modified when the reorientation of the approaching deformed projectile in the Coulomb field is taken into account. A model is developed which is an extension of the 3S-CMD model and which can be used for three or many-body systems [41].

Weakly-bound nucleus can be constructed as a cluster of two or more rigid nuclei such that the entire cluster has the properties of the corresponding nucleus. Interaction between the fragments is generated self-consistently and both the projectile and the target are extended objects with desired size and shape deformation. Relaxation of the rigid-body constraint at appropriate stages takes care of excitation of the target and the projectile fragments.

Initially, the target plus the clustered projectile system is placed along the Rutherford trajectories for a given initial condition. All the rigid bodies move under the influence of the ion–ion potential and the torques generated by the interaction. Coupled classical

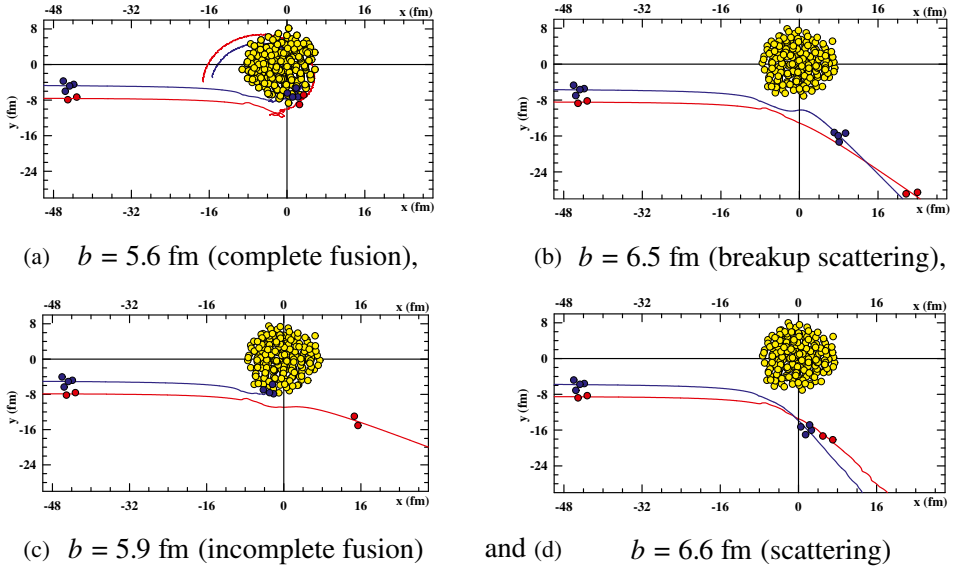

(a) b = 5.6 fm (complete fusion), (b) b = 6.5 fm (breakup scattering),

(c) b = 5.9 fm (incomplete fusion) and (d) b = 6.6 fm (scattering)

Figure 10. ^{6}Li + ^{209}Bi collision at $E_{\rm cm}$ = 42.7 MeV [41].

equations of motion can be numerically solved to obtain the trajectories of the respective centre of mass and orientation of the principle axes of the respective rigid bodies.

The weakly-bound ^{6}Li projectile is constructed as a cluster of ^{2}H and ^{4}He. The potential energy (−1.446 MeV) between them corresponds to the experimentally observed

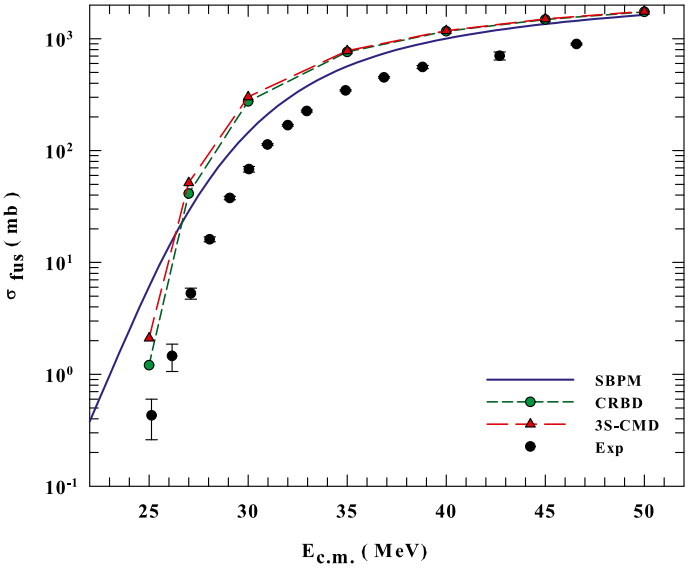

Figure 11. Fusion cross-section for ^{6}Li + ^{209}Bi system.

breakup threshold energy. Figure 10 shows the ^{6}Li+^{209}Bi collision at $E_{\rm cm} = 42.7$ MeV and different impact parameters [41]. This figure demonstrates all types of possible reactions between the projectile and the target in the model simulation. Thus, the model looks promising for studying heavy-ion fusion involving weakly-bound projectiles.

Initial calculation of complete fusion cross-sections for ^{6}Li+^{209}Bi reaction in 3-body 3S-CMD model, where rigid-body constraints are completely relaxed for the target, both the projectile fragments, and the ^{2}H–^{4}He cluster in ^{6}Li, are shown in figure 11 . The results are also compared with the SBPM and CRBD model calculations.

8. Summary

Classical microscopic models with various levels of degrees of freedom are discussed. The nuclei used in these models were constructed using a potential energy minimization code STATIC and a soft-core Gaussian form of *NN* potential with suitable choice of potential parameters. The SBPM model assumes the colliding nuclei to be rigid and also assumes a sudden approximation which corresponds to freezing of all the internal degrees of freedom including the rotational ones. The size and shape of the nuclei are reflected in the orientation-averaged fusion cross-sections and the distribution of barriers.

Allowing the rotational and translational degrees of freedom through rigid-body equations of motion in the CRBD model demonstrated the effect of long-range Coulomb torque on the deformed colliding partner. These calculations show the importance of initiating the dynamical evolution from large initial separations. The calculations also show that the barrier parameters are not only dependent on the initial orientations but also on the collision energy and the moment of inertia. The usual CMD calculations are modified and combined with the CRBD stage in a 3S-CMD model, which then takes care of the reorientation effect arising from long distances and the internal excitations of the target/projectile nuclei at short distances in a single model calculation.

The weakly-bound projectile breakup reactions are simulated by assuming the projectile to be made up of a weakly-bound cluster of two stable nuclei in a 3-body 3S-CMD approach. All the essential features of breakup reactions such as complete fusion, incomplete fusion, no-capture breakup and scattering are demonstrated.

Acknowledgement

A part of the work reported here was carried out with the financial assistance under a DAE–BRNS Project No. 2009/37/20/BRNS. The author thanks M R Morker for help with computing for some of the results.

References

[1] M Dasgupta *et al*, *Annu. Rev. Nucl. Part. Sci.* **48**, 401 (1998) and references therein
[2] V Yu Denisov and N A Pilipenko, *Phys. Rev. C* **76**, 014602 (2007)
[3] J R Birkelund *et al*, *Phys. Rep.* **56**, 107 (1979)
[4] K Hagino, N Rowley and A T Kruppa, *Comput. Phys. Commun.* **123**, 143 (1999)

[5] A B Balantekin and N Takigawa, *Rev. Mod. Phys.* **70**, 77 (1998)
[6] N Chauhan and S S Godre, *Proc. Symp. Nucl. Phys.* **56**, 640 (2011)
[7] C Simenel, Ph Chomaz and G de France, *Phys. Rev. Lett.* **93**, 102701 (2004)
[8] C Simenel *et al*, arXiv:nucl-th/0605018v1 (2006)
[9] A S Umar and V E Oberacker, *Phys. Rev. C* **74**, 024606 (2006)
[10] P Bonche *et al*, *Nucl. Phys. A* **443**, 39 (1985)
[11] K Washiyama and D Lacroix, *Phys. Rev. C* **78**, 024610 (2008)
[12] V E Oberacker *et al*, *Phys. Rev. C* **82**, 034603 (2010)
[13] A R Bodmer and C N Panos, *Phys. Rev. C* **15**, 1342 (1977)
[14] J J Molitoris *et al*, *Phys. Rev. Lett.* **53**, 899 (1984)
[15] S M Kiselev, *Phys. Lett. B* **154**, 247 (1985)
[16] Y Kitazoe, K Yamamoto and M Sano, *Lett. Nuovo Cimento* **32**, 337 (1981)
[17] A Vicentini, G Jacucci and V R Pandharipande, *Phys. Rev. C* **31**, 1783 (1985)
[18] V S Rammurthy and S K Kataria, *Pramana – J. Phys* **11**, 457 (1978)
[19] A N Dixit, V S Ramamuthy and Y R Waghmare, *Pramana – J. Phys.* **20**, 523 (1983)
[20] S S Godre and P R Desai, *Nucl. Phys. A* **834**, 195 (2010)
[21] P R Desai, *Effect of Coulomb reorientation on fusion cross-sections and barrier distributions of some heavy-ion reactions*, Ph.D. Thesis (Veer Narmad South Gujarat University, 2009)
[22] P R Desai and S S Godre, *Proc. Int. Symp. Nucl. Phys.* **54**, 294 (2009)
[23] H Holm and W Greiner, *Phys. Rev. Lett.* **26**, 1647 (1971)
[24] H D Marta, L F Canto and R Donangelo, *Phys. Rev. C* **78**, 034612 (2008)
[25] A Diaz-Torres *et al*, *Phys. Rev. Lett.* **98**, 152701 (2007)
[26] S S Godre and Y R Waghmare, *Phys. Rev. C* **36**, 1632 (1987)
[27] S S Godre, *Nucl. Phys. A* **734**, E17 (2004)
[28] P R Desai and S S Godre, *Eur. Phys. J. A* **47**, 146 (2011)
[29] Y R Waghmare, *Phys. Rev. B* **136**, 1261 (1964)
[30] W D Myers and W J Swiatecki, *Ann. Phys. (N.Y.)* **55**, 395 (1969)
[31] S S Godre, *Proc. Symp. Nucl. Phys. B* **32**, 10 (1989)
[32] I B Desai and S S Godre, *Proc. Int. Symp. Nucl. Phys.* **54**, 196 (2009)
[33] S S Godre and P R Desai, *Proc. Symp. Nucl. Phys.* **53**, 341 (2008)
[34] C Y Wong, *Phys. Rev. Lett.* **31**, 766 (1973)
[35] S S Godre, *Proc. Symp. Nucl. Phys. B* **35**, 268 (1992)
[36] S S Godre, *Proc. Symp. Nucl. Phys. B* **39**, 192 (1996)
[37] S S Godre, *Proc. Symp. Nucl. Phys. B* **42**, 224 (1999)
[38] A J Maciejewski, *Celest. Mech. Dyn. Astron.* **63**, 1 (1995)
[39] M R Morker and S S Godre, *Proc. Symp. Nucl. Phys.* **57**, 560 (2012)
[40] K Hagino *et al*, *Phys. Rev. C* **61**, 037602 (2000)
[41] M R Morker and S S Godre, *Proc. Symp. Nucl. Phys.* **56**, 644 (2011)